Virology 418 (2011) 102–112

Contents lists available at ScienceDirect

Virology

journal homepage: www.elsevier.com/locate/yviro

Cowpox virus infection of cynomolgus macaques as a model of hemorrhagic smallpox

Reed F. Johnson [a,*], Srikanth Yellayi [b], Jennifer A. Cann [b], Anthony Johnson [b], Alvin L. Smith [a], Jason Paragas [b], Peter B. Jahrling [a,b], Joseph E. Blaney [a]

[a] Emerging Viral Pathogens Section, National Institute of Allergy and Infectious Diseases, National Institutes of Health, Bethesda, MD 20892, USA
[b] Integrated Research Facility, National Institute of Allergy and Infectious Diseases, National Institutes of Health, Frederick, MD 21702, USA

ARTICLE INFO

Article history:
Received 18 May 2011
Returned to author for revision 15 July 2011
Accepted 18 July 2011
Available online 15 August 2011

Keywords:
Orthopoxvirus
Animal model
Cowpox virus
Variola virus
Smallpox
Hemorrhagic disease
Pathogenesis

ABSTRACT

Hemorrhagic smallpox was a rare but severe manifestation of variola virus infection that resulted in nearly 100% mortality. Here we describe intravenous (IV) inoculation of cowpox virus Brighton Red strain in cynomolgus macaques (*Macaca fascicularis*) which resulted in disease similar in presentation to hemorrhagic smallpox in humans. IV inoculation of macaques resulted in a uniformly lethal disease within 12 days post-inoculation in two independent experiments. Clinical observations and hematological and histopathological findings support hemorrhagic disease. Cowpox virus replicated to high levels in blood (8.0–9.0 $\log_{10}$ gene copies/mL) and tissues including lymph nodes, thymus, spleen, bone marrow, and lungs. This unique model of hemorrhagic orthopoxvirus infection provides an accessible means to further study orthopoxvirus pathogenesis and to identify virus-specific and nonspecific therapies. Such studies will serve to complement the existing nonhuman primate models of more classical poxviral disease.

Published by Elsevier Inc.

Introduction

The threat of intentional release of variola virus (VARV), the causative agent of smallpox, continues to be a chief biodefense concern as the proportion of the world population without prior vaccination expands. The most common form of disease, classical smallpox, was associated with a case fatality rate of 30% in unvaccinated individuals, thereby constituting a grave concern for public health if VARV is re-introduced. Zoonotic orthopoxviruses including cowpox (CPXV) and particularly monkeypox virus (MPXV) currently cause sporadic disease in humans (Parker et al., 2007; Vorou et al., 2008), with case-fatality rates from MPXV infections reaching as high as 10% (Jezek et al., 1983, 1988; Likos et al., 2005). (Rimoin et al., 2010) recently described a considerable increase in the incidence of MPXV in the Democratic Republic of Congo. Based on the above considerations, investigations into orthopoxviral pathogenesis and the identification of countermeasures have accelerated over the past decade (Chapman et al., 2010; Earl et al., 2008; Huggins et al., 2009; Jahrling et al., 2004; Sbrana et al., 2007).

The development of animal models that accurately reflect human disease is critical to our understanding of the pathogenesis of VARV infection and evaluation of countermeasures against the orthopoxviruses. Because of the successful eradication of smallpox and the sporadic and geographically isolated nature of MPXV outbreaks, the only option for licensing new drugs and vaccines for smallpox and other orthopoxvirus diseases is extrapolation of data derived from accurate, validated animal models (Anon., 2009; Geisbert and Jahrling, 2004; Kramski et al., 2010; Sullivan et al., 2000). The "Animal Rule" requires that a countermeasure be evaluated in at least 2 animal models in which the route and dose of virus administration, time to onset of disease, and time course/progression of disease optimally mimic the pathophysiology of the human disease. While VARV and MPXV nonhuman primate (NHP) models in cynomolgus and rhesus macaques have been used successfully for evaluation of vaccines and antiviral therapies (Earl et al., 2004, 2008; Edghill-Smith et al., 2005a,b; Hooper et al., 2004; Jahrling et al., 2005; Sbrana et al., 2007; Stittelaar et al., 2001, 2005, 2006), biosafety and security restrictions on the use of both viruses limit their widespread use by the research community. MPXV experimentation requires Centers for Disease Control and Prevention (CDC) Select Agent registration and biosafety laboratory (BSL)-3 containment. VARV research is highly restricted to BSL-4 containment at the CDC in the United States or the State Research Center of Virology and Biotechnology (Vector) in Russia and requires World Health Organization approval. In addition to the need for animal models that accurately reflect all manifestations of smallpox, the future of VARV research is uncertain due to increasing international political interest in eradication of known VARV stocks (Lane and Poland, 2011; McFadden, 2010; Tucker, 2011). Therefore,

* Corresponding author at: NIH/NIAID/EVPS, Bldg 33, Rm 2E19A, 33 North Drive, Bethesda, MD 20892, USA. Fax: +1 301 480 3322.
E-mail address: johnsonreed@mail.nih.gov (R.F. Johnson).

0042-6822/$ – see front matter. Published by Elsevier Inc.
doi:10.1016/j.virol.2011.07.013

an NHP model that mimics VARV induced disease and is readily available to the broader research community would serve as a distinct advantage to accelerate research and complement or if necessary, potentially replace the VARV NHP model for efficacy studies of countermeasures.

In contrast to VARV or MPXV, CPXV can be studied under BSL-2 laboratory conditions and does not require Select Agent registration. CPXV is known to be highly virulent in mice, and intraperitoneal, intranasal, and aerosol routes of administration have been used to study the efficacy of antivirals (Bray and Buller, 2004; Smee et al., 2008). Recently, outbreaks of CPXV disease in NHPs housed in European zoos have been reported, and lethal disease was reported in common marmosets (Martina et al., 2006; Matz-Rensing et al., 2006). Experimental studies using the isolated CPXV strain determined that the lethal $dose_{50}$ via intranasal inoculation in marmosets was $<10^3$ PFU and that the strain produced some typical signs of poxviral disease (Kramski et al., 2010). While establishing the marmoset infection model was significant, previous orthopoxvirus research has predominantly used macaque species (Chen et al., 2005; Earl et al., 2008; Edghill-Smith et al., 2005a; Hooper et al., 2004; Huggins et al., 2009; Jahrling et al., 2004; Stittelaar et al., 2001) and critical reagents are readily available for macaques. To compare CPXV-induced disease to the established macaque models of VARV and MPXV, more extensive analysis of CPXV in macaques is required.

Here we demonstrate that intravenous (IV) inoculation of CPXV Brighton Red strain in cynomolgus macaques (*Macaca fascicularis*) resulted in severe hemorrhagic disease with rapid mortality using an inoculum as low as 5×10^5 PFU. Clinical, hematological, and histopathological analysis provided evidence for hemorrhagic disease with similarities to both the NHP model of VARV infection (Jahrling et al., 2004) and human hemorrhagic smallpox. While hemorrhagic smallpox was a rare manifestation of disease (<3% of cases), it was rapid, severe, and nearly uniformly fatal (Dixon, 1962; Downie et al., 1969; Fenner, 1988a). These findings represent the first step in developing CPXV infection in macaques as a model to complement existing orthopoxvirus models.

Results

CPXV infection results in a rapid and lethal disease with hemorrhagic manifestations

Fourteen cynomolgus macaques were inoculated intravenously with 10-fold dilutions of CPXV in two independent experiments; experiment one comprised one dosage group of 5×10^7 PFU (n=3) and experiment two comprised three dosage groups of 5×10^7 PFU (n=3), 5×10^6 (n=4), and 5×10^5 (n=4). Except where noted, all 6 NHPs receiving 5×10^7 PFU CPXV are included for analysis. Infection resulted in a fulminant disease with hemorrhagic manifestations that was dose-independent. Clinical signs of disease included depression, lethargy, inappetence, ecchymoses, petechia, weakness, hematuria, and proteinura. Less common clinical signs were diarrhea, melena, and weight loss. Typical poxviral exanthema and enanthema developed and are described below (Table 1). NHPs became moribund and reached clinical endpoint criteria for euthanasia as described in the Materials and methods between days five and twelve post-inoculation.

Gross and histopathological findings indicate severe hemorrhagic disease

Comprehensive postmortem examinations were performed when NHPs met endpoint criteria on days 5, 5, 6, 6, 7, and 11 for the 5×10^7 PFU group; days 7, 8, 8, and 9 for the 5×10^6 PFU group; and days 7, 7, 10, and 12 for the 5×10^5 PFU group (Table 1). The classic hallmarks of orthopoxvirus infection, exanthema and enanthema (Jezek et al., 1987b; Martin, 2002), were less numerous in NHPs infected with CPXV compared to other orthopoxvirus NHP models (Jahrling et al., 2004; Johnson et al., 2011). Lesions developed in 9 of 14 NHPs, but peak lesion counts (Table 1) were below levels typically observed in MPXV or VARV infection (Fenner, 1988a; Huggins et al., 2009; Johnson et al., 2011; Ricketts, 1910; Stittelaar et al., 2005, 2006). Cutaneous and mucosal lesions developed on the face, extremities, thorax, abdomen, oral mucosa, pharynx, and anogenital region, and often appeared hemorrhagic (Fig. 1A). In addition, cutaneous erythema and ecchymoses, independent of vesicular lesions, were common (Fig. 1B). Other gross findings included lymph node hemorrhage and edema (Fig. 1C), multifocal petechial hemorrhages on the mucosal surface of the gastrointestinal tract (Fig. 1D), and multifocal petechial hemorrhages on heart, lungs, kidneys, urinary bladder, and brain (data not shown).

Histopathological evaluation confirmed severe hemorrhagic involvement of multiple components of the skin and mucous membranes, with no correlation between inoculation dose and lesion severity or distribution. Skin and mucous membrane changes included typical intraepidermal vesicles, swollen keratinocytes (ballooning degeneration) with intracytoplasmic inclusion bodies, ulceration, and dermal/submucosal hemorrhage and edema. Similar to other chordopoxviruses, the inflammatory cellular infiltrate ranged from neutrophilic infiltrate within the stratum corneum of the epidermis (subcorneal pustules) to a mononuclear infiltrate within the vesicular lesions of the epidermis. Secondary lymphoid organs including spleen, lymph node, and tonsil were often severely affected, and changes included necrotizing tonsillitis, lymphoid necrosis and depletion, sinusoidal edema, hemorrhage, and fibrin deposition occurring in 14/14 NHPs and intralesional bacteria occurring in 6/14 NHPs (Figs. 2A and B). Immunohistochemical (IHC) staining frequently revealed viral antigen in lymph nodes and spleen (Figs. 3A and B). In 3/14 NHPs, severe diffuse hematopoietic necrosis with hemorrhage, congestion, and intralesional bacteria was found (Fig. 2C). As in the lymphoid organs, necrotic areas of bone marrow were positive for poxviral antigen as assessed immunohistochemically (Fig. 3C). Examination of the heart revealed multifocal lymphohistiocytic myocarditis in all NHPs with myofiber degeneration necrosis, vascular congestion and hemorrhage (Fig. 2D); immunohistochemically, viral antigen was present in mononuclear cells within the interstitium (Fig. 3D).

Other findings included interstitial pneumonia (14/14 NHPs), interstitial nephritis (14/14 NHPs), and hepatitis (14/14 NHPs). Viral antigen staining was sporadically found in mononuclear cells within the renal interstitium and glomeruli. 3/14 NHPs were found to be positive for bacteria in the blood by culturing blood samples on blood and chocolate agar at necropsy, although no further testing was performed to definitively identify the bacteria. In 6/14 NHPs (including the 3 positive by culturing blood), intralesional colonies of Gram positive or Gram negative bacteria were found in 5 or more different organs indicating concurrent development of a secondary bacterial infection.

Hematological analyses indicate signs of hemorrhage and coagulopathy

Red blood cell count, hematocrit, and hemoglobin concentrations were monitored periodically pre- and post-inoculation (Figs. 4A–C). All 3 parameters decreased dramatically during the course of infection, consistent with the observed hemorrhagic signs. The development of anemia was not dose-dependent and appeared consistently by day 5 or at the time of moribund endpoint. Concurrent with the development

Table 1
Survival and lesion count of NHPs infected with cowpox virus.

Dose (PFU)	Group size	Survival (%)	Mean day of endpoint (range)	Peak lesion count (range)	Mean day of lesion onset (range)
5×10^5	4	0	9.0 (7–12)	103 (0–306)	9.0 (8–10)
5×10^6	4	0	8.0 (7–9)	6 (0–13)	8.0 (n/a)
5×10^7	6	0	6.7 (5–11)	76 (0–184)	4.2 (3–8)

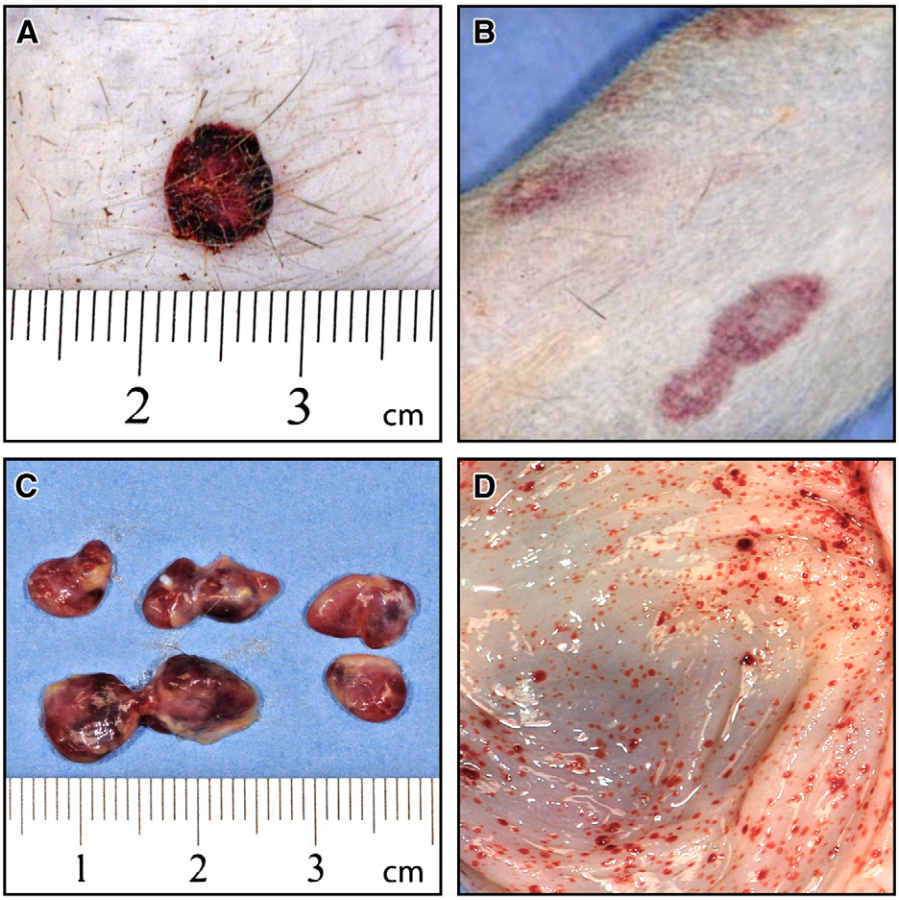

Fig. 1. Gross pathology of CPXV-infected NHPs indicates a systemic hemorrhagic disease. A. Hemorrhagic skin lesion. B. Ecchymoses on skin. C. Hemorrhage and edema of lymph nodes. D. Petechiae on gastrointestinal tract mucosa (stomach).

of anemia was the development of several signs of disseminated intravascular coagulation (DIC). Specifically, thrombocytopenia, elevated PT, and increased FDP and D-dimer concentrations in serum were detected (Figs. 4D–H). Thrombocytopenia was the only evaluated hemostatic parameter that may be dose-dependent (Fig. 4D). PT increased in 9 of 11 NHPs and typically peaked at endpoint (Fig. 4F). Further support for DIC included elevations in the concentration of FDPs (Fig. 4G) and D-dimers (Fig. 4H) that were detected in the serum of 13 of 14 NHPs. Mean peak D-dimer concentrations increased approximately 1000-fold from baseline across the dosage groups. Interestingly, aPTT decreased in 7/11 NHPs, remained within normal range in 3 NHPs, and increased in a single NHP inoculated with 5×10^5 PFU that survived to day 12 (Fig. 4E).

PBMC analysis indicates expansion of adaptive immune cells and depletion of innate immune cells

Concentrations of CD14+ (monocytes), CD16+ (NK cells), CD4+ (helper T-cell), CD8+ (killer T-cell), and CD20+ (immature B-cell) cell populations were assayed by TruCount methodology as described in the Materials and methods at periodic blood draws and at moribund endpoint. Analysis of the PBMC profiles revealed two patterns that were consistently observed across dosage groups (Fig. 5). First, circulating CD14+ and CD16+ cells were largely depleted as NHPs met moribund endpoint criteria with the exception of a single NHP in the 5×10^6 PFU group which had an elevated level of CD14+ cells. Preceding this decline in innate immune cell populations, two-fold or greater increases in CD14+ or CD16+ cell concentrations were observed in 9/11 and 5/11 NHPs, respectively, indicating an initial pro-inflammatory response. Second, further support for the pro-inflammatory response was provided by the consistent elevation of adaptive immune cells. Specifically, 10/11 NHPs had two-fold or greater rises in circulating CD4+, CD8+, and CD20+ cell populations at late stages of the disease course. In NHPs that survived past day 8 in the 2 lower dosage groups, relative declines in CD4+, CD8+, and CD20+ cell populations to pre-infection concentrations were observed. Using a flow cytometric neutralizing antibody assay, we were unable to detect any neutralizing antibody activity in the CPXV-infected NHPs (data not shown). Specific T cell responses were not assayed.

Cytokine/chemokine response to hemorrhagic CPXV infection

The pro-inflammatory cytokines/chemokines monocyte chemoattractant protein-1 (MCP-1 or CCL2), interleukin-6 (IL-6), IL-8, and interferon-γ (IFN-γ) were previously reported to be elevated in VARV-infected NHPs that developed hemorrhagic disease and were therefore a focus in this study (Fig. 6) (Jahrling et al., 2004). MCP-1 and IL-8 concentrations rose in the majority of NHPs after days 3–4 post-inoculation in CPXV-infected NHPs in a dose-independent manner and typically did not start to increase until after days three to four. However, two NHPs in the 5×10^7 PFU group reached peak concentrations of MCP-1 at day four post-infection which was maintained in 1 NHP until endpoint criteria were met. In contrast, elevations in IL-6 concentrations were suggestive of dose-dependence. IFN-γ concentrations followed a different pattern of activation, with peak values reached in the 5×10^6 PFU and 5×10^7 PFU groups primarily between days 3 and 4 followed by a decrease in concentrations prior to moribund endpoint. Elevations of IFN-γ concentrations in the 5×10^5 PFU group were less pronounced. Peak concentrations for MCP-1 (14/14 NHPs), IL-6 (10/14 NHPs), and IL-8 (13/14 NHPs) coincided with endpoint.

Several additional cytokines, including IL-1-receptor antagonist (IL-1ra), IL-18, RANTES, soluble CD40 ligand (sCD40L), granulocyte colony stimulating factor (G-CSF), and vascular endothelial growth factor (VEGF) were also elevated after CPXV infection (Table 2). IL-1ra, IL-18, and VEGF had the highest and most consistent elevations between the groups and peak concentrations coincided with moribund endpoint suggesting their importance in disease outcome. No significant changes were identified for levels of granulocyte macrophage colony stimulating factor (GM-CSF), macrophage inflammatory protein-1 α and β (MIP-1α, MIP-1β), IL-1β, IL-2, IL-4, IL-5, IL-10, IL-12, IL-13, IL-15, IL-17, transforming growth factor-α (TGF-α), or tumor necrosis factor-α (TNF-α).

CPXV replication was observed in multiple organ systems

Viral load in the blood as measured by qPCR (viremia) and oral and nasal swabs indicated CPXV replication that was largely dose-independent (Table 3). Mean peak viremia ranged from 8.4 to 9.1 $\log_{10}$ gene copies/mL across the dosage groups and coincided with moribund endpoint for 10/13 NHPs evaluated (data not shown). Virus shed from oral and nasal mucosa was detected as early as day three/four post-infection in all NHPs and similarly peaked at the time of endpoint.

At the time of necropsy, tissue homogenates were isolated from 41 tissues and assayed for viral load by plaque assay. As expected, CPXV widely disseminated and commonly reached virus titers of greater than 6.0 $\log_{10}$ PFU/g of tissue or greater (Fig. 7). Lymphoid tissues, including spleen, lymph node, thymus, and tonsil, and bone marrow were typical sites of high CPXV replication, consistent with previous orthopoxvirus studies (Johnson et al., 2011; Jordan et al., 2009). Additional sites of high viral loads included the nares, lungs, liver, kidneys and adrenal glands.

Discussion

The present study indicates that infection of cynomolgus macaques with CPXV Brighton Red may be a suitable model for hemorrhagic smallpox. Hemorrhagic smallpox was the most severe clinical presentation of VARV infection in humans, resulting in almost 100% lethality. To date, the only macaque model of hemorrhagic orthopoxvirus disease requires IV inoculation of 1×10^9 PFU of VARV into cynomolgus macaques (Jahrling et al., 2004). However, variola research is highly restricted, and the high virus titer (10,000-fold higher than the lowest lethal dose reported here) required to induce uniformly lethal disease indicates the need for additional models of orthopoxvirus infection. Development of improved NHP orthopoxvirus models must rely on expanding what has been learned from IV inoculation models, because, although IV inoculation does not reproduce natural transmission and essentially skips the prodromal phase of disease, it repeatedly results in fulminant disease characteristic of severe classical pox-like disease and has been used to successfully evaluate anti-orthopoxvirus therapeutics and vaccines (Earl et al., 2004, 2007, 2008; Edghill-Smith et al., 2005a,b; Huggins et al., 2009; Stittelaar et al., 2001, 2005, 2006). Improvements in MPXV disease modeling have come from studies of airway and respiratory exposure routes including aerosol, intrabronchial, and intratracheal, but these methods may be hampered by exaggerated respiratory disease, decreased lesional disease, and variable disease presentation and outcome (Goff et al., 2011; Johnson et al., 2011; Zaucha et al., 2001). Therefore, while intravenous inoculation is imperfect, it is a viable method to test the efficacy of countermeasures under an extreme form of viral challenge. There is no current indication that a countermeasure that protects against intravenous challenge and its associated rapid, fulminant disease would fail against respiratory challenge which may result in slower disease progression. However, further development of respiratory models is clearly warranted.

Investigation of CPXV as a model of human smallpox is supported by analysis of the data reviewed by (Seet et al., 2003) that indicates that VARV and CPXV share 19 immunomodulatory genes based on function. CPXV encodes 3 additional proteins when compared to VARV, all targeting the TNF-α pathway (CrmC, CrmE, and CrmD). By comparison MPXV shares 14 immunomodulatory genes with VARV with 2 proteins not shared with VARV, CrmE (a TNF-α pathway inhibitor) and CD-46, a

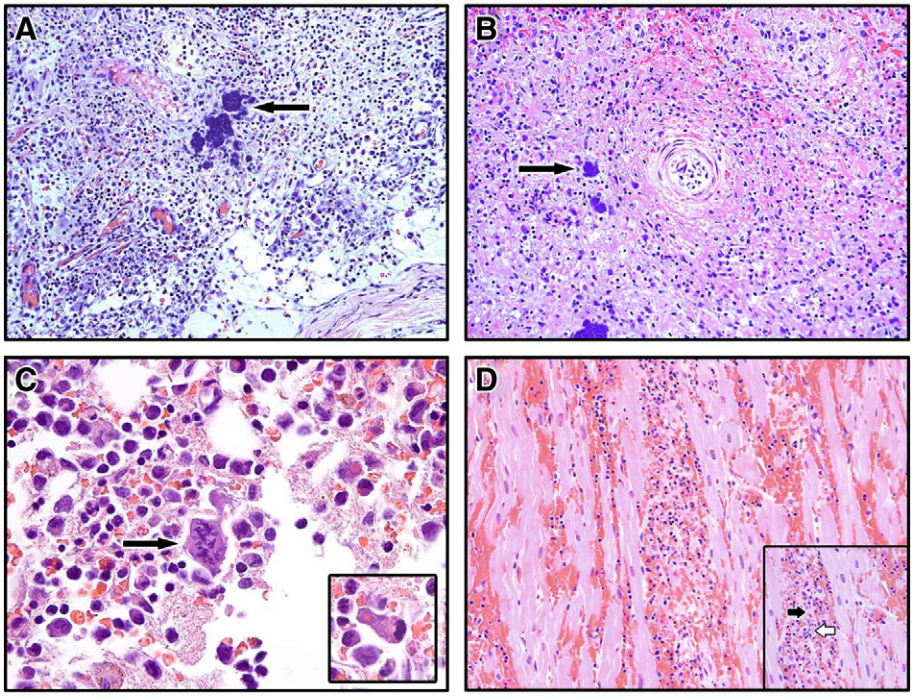

Fig. 2. Hematoxylin and eosin staining of lymph node, spleen, bone marrow, and the heart collected at necropsy from CPXV-infected NHPs. (A) Lymph node (20×): necrosis, edema and intralesional bacteria (arrow). (B) Spleen (20×): diffuse necrotizing splenitis with hemorrhage, fibrin and intralesional bacteria (arrow). (C) Bone marrow (40×): hypocellular with necrosis, intracellular bacteria (arrow). Inset: viral intracytoplasmic inclusion. (D) Heart (20×): lymphohistiocytic myocarditis with myofiber degeneration, hemorrhage, and non-suppurative myocarditis. Inset: the black arrow indicates myocardial necrosis, white arrow indicates lymphohistiocytic infiltration of the myocardium.

complement inhibitor (Seet et al., 2003). Phylogenetic analysis also suggests that, depending upon methodology, CPXV may be more closely related to VARV than MPXV (Gubser et al., 2004; Lefkowitz et al., 2005; Xing et al., 2006). For example, (Gubser et al., 2004) demonstrated that by the maximum-likelihood method using nucleotide sequences that CPXV-Brighton Red is more closely related to VARV than MPXV. In contrast Xing et al. demonstrated by gene sequence homology based on most parsimonious trees using amino acid sequence of 49 shared genes that MPXV and CPXV were more closely related to each other than either was to VARV. Analysis of the same 49 shared genes by the neighbor-joining tree method indicated that MPXV was more closely related to VARV than was CPXV (Xing et al., 2006). While high sequence homology of a surrogate orthopoxvirus is a chief consideration in model development, it should be noted that the similarity of disease presentation in the animal model may be equally as important in the demonstration of countermeasure efficacy.

Clinical presentation of hemorrhagic CPXV disease after IV inoculation of CPXV shares several features with hemorrhagic smallpox in humans. Clinical signs such as increased PT, increased D-dimers, FDP, and thrombocytopenia indicating DIC were similar to the coagulation disorders reported in human hemorrhagic smallpox (Haviland, 1952; McKenzie et al., 1965; Roberts et al., 1965). Although increased aPTT is often associated with DIC, decreases in aPTT can occur in DIC as part of the initial acute phase reaction (Favaloro, 2010). Gross observations such as erythematous, petechial, and hemorrhagic lesions involving the face, oronasal cavities, thoraco-abdominal and anogenital regions, and upper torso of NHPs in this study resemble the erythema, petechiae, and hemorrhage on the mouth, oral cavity, arms, and trunk observed in patients with hemorrhagic smallpox (Bras, 1952; Haviland, 1952; McKenzie et al., 1965; Rao, 1964; Roberts et al., 1965). Histopathologic similarities in examined tissues included: hemorrhage, lymphoid depletion, hepatocyte necrosis, and hypocellularity of the bone marrow observed in the present study (Bras, 1952; Councilman et al., 1904a; Martin, 2002). Bacteremia, which likely contributed to disease, was commonly observed in both human hemorrhagic smallpox and CPXV infection described here (Councilman et al., 1904b; Kempton and Parsons, 1920; Ricketts, 1910). Death or moribund endpoint occurred within 5–12 days post exposure in both conditions. We note that in CPXV-infected marmosets, (Kramski et al., 2010) observed focal hemorrhages near lesion sites as well as petechiation of the larynx and parts of the thorax, but there was no indication of systemic hemorrhagic disease as described here.

Differences were also observed between human hemorrhagic smallpox and experimental CPXV-induced disease. Fewer cutaneous lesions were observed during CPXV-induced disease than what was observed in patients with hemorrhagic smallpox (Fenner, 1988a; Martin, 2002) and VARV-inoculated NHPs (Jahrling et al., 2004). Interestingly, human cases of CPXV are often characterized by a single or few lesions suggesting that fewer cutaneous lesions are a common feature in humans (Baxby et al., 1994) and NHPs. Cardiac changes in human hemorrhagic smallpox included multifocal myocardial and subendocardial hemorrhage (Bras, 1952; Lillie, 1930). Lymphohistiocytic myocarditis, as was seen in this study, was also reported in human smallpox but this lesion was not classified by disease type (Bras, 1952; Councilman et al., 1904a; Fenner, 1988b). Fever was also only observed in 2/14 NHPs in this study while fever was often more severe in hemorrhagic smallpox when compared to classical smallpox indicating an apparent difference between this model and human disease (Councilman et al., 1904b; Ricketts, 1910). Although temperature increases were observed in NHPs it is unknown if the observed increase is affected by anesthesia, and it is also possible that a short lived fever would not be observed due to the physical exam schedule. Alternatively, it is possible that cowpox modulates IL-1 receptor signaling resulting in lack of fever response by the NHPs. Telemetry may be implemented as part of future studies to gather meaningful data to determine the role of fever in this CPXV model.

Direct comparison between cytokine concentrations in human hemorrhagic smallpox and CPXV cannot be performed because cytokine data from human cases has not been reported. IL-6, IL-8, and MCP-1 have been implicated in responses that may promote coagulation disorders in other diseases (Charo and Taubman, 2004; Huerta-Zepeda et al., 2008; Johnson et al., 1998; Levi and van der Poll, 2010) and high

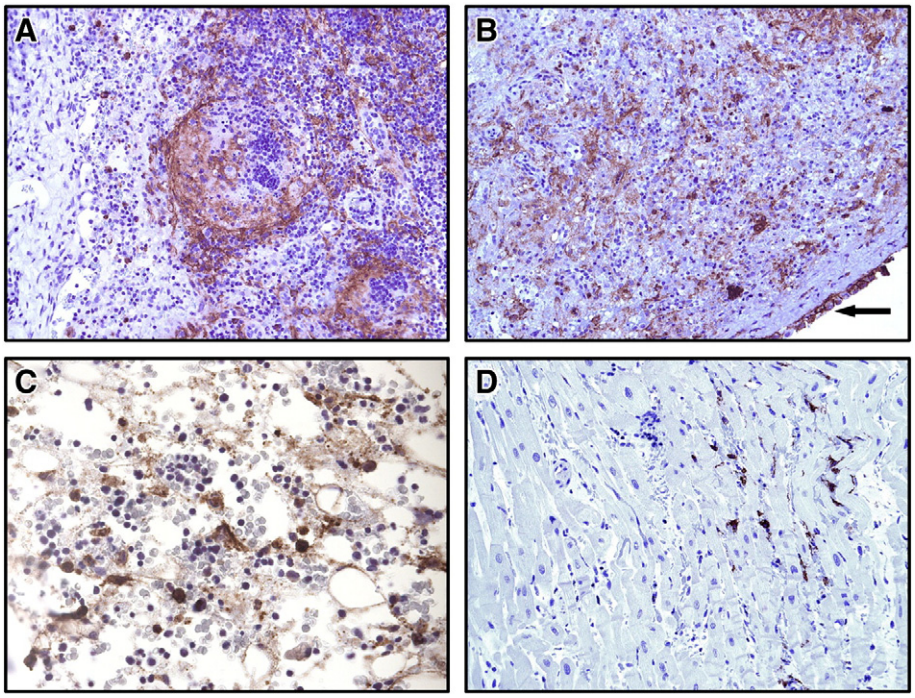

Fig. 3. Immunohistochemistry of lymph node, spleen, bone marrow and heart collected at necropsy using cross-reactive anti-vaccinia virus staining. (A) Lymph node (20×): follicular and paracortical poxvirus antigen staining. (B) Spleen (20×): diffuse poxvirus antigen within areas of necrosis and capsular mesothelium (arrow). (C) Bone marrow (40×): hypocellularity with immunopositive myeloid cells within areas of necrosis. (D) Heart (20×): immunopositive mononuclear cells within the interstitium.

concentrations of MCP-1 and IL-6 have been shown to increase tissue factor expression (Charo and Taubman, 2004; Levi and van der Poll, 2010) which may help initiate the extrinsic coagulation cascade. Our cytokine and chemokine analysis indicated a pro-inflammatory response with elevations in MCP-1, IL-18, and IFNγ. MCP-1, IL-6 and IFNγ were of particular interest because they were elevated in NHPs inoculated with VARV Harper (Jahrling et al., 2004). However, during CPXV infection IL-8 and IL-6 did not increase in all NHPs suggesting that they may play a limited role in CPXV induced disease.

Comparison of cytokine concentrations in NHPs inoculated with 5×10^7 PFU IV MPXV (dose with highest lethality) to CPXV revealed similar peak fold changes of 1.3, 1.6, and 1.9-fold for MCP-1, IL-6, and IL-8, respectively. In contrast, during MPXV infection, IFNγ increases 400-fold and only 21-fold in CPXV inoculated NHPs across all 3 doses reported here. IL-18 was not elevated in MPXV but was elevated on average 460-fold across all 3 doses in CPXV inoculated NHPs. The data suggests a complex interplay between cytokines and chemokines involving concentrations relative to each other, timing of induction, and combinations of cytokines that may partly determine disease presentation and outcome. When compared to Ebola hemorrhagic fever in humans, several similarities exist: IL-4 is not abundantly expressed in either disease. However, RANTES, IL-6, and IL-8 demonstrated approximately 6 fold (500 pg/mL peak average), 10 fold (1000 pg/mL peak average), and 10 fold (500 pg/mL peak average) increases in nonsurvivors when compared to survivors of SEBOV infection. During Zaire Ebola Virus (ZEBOV) infection IL-6, IL-8, and MCP-1 demonstrated approximately 1.5 (100 pg/mL peak average) fold, 15 fold (1000 pg/mL peak average), and 7.5 fold (750 pg/mL peak average) increases in concentrations in ZEBOV induced disease. Differences include a 10 fold increase in TNFα expression in Ebola-infected humans and no significant upregulation of IFNγ (Hutchinson and Rollin, 2007; Wauquier et al., 2010).

The lymphoid pathogenesis and decline in innate immune cells observed during CPXV infection may provide a unique opportunity to identify the impact of the mononuclear phagocytic and lymphoid systems in orthopoxvirus disease progression. The observed decline in the innate immune cells present in the PBMC population may be the result of either the loss of progenitor hematopoietic cells or direct viral cytopathic effects within the monocyte–macrophage system and lymphoid system, either of which would exacerbate disease. Bone marrow hypocellularity could represent the loss of precursor pluripotent cells due to direct lytic infection by CPXV or an indirect effect of infection, but the cause of such changes is unknown. In animals that survived past day 8, CD14+, CD16+, CD4+, CD8+, and CD20+ cell populations sharply declined prior to moribund endpoint. Disruption of the bone marrow and lymphoid tissue likely plays a key role in disease outcome because these PBMC cell populations are ultimately replenished from the bone marrow and undergo maturation in lymphoid tissue. Further investigations with this model may help delineate the role of the individual PBMC populations in disease progression.

Immunosuppression presumably played a role in the development of secondary bacterial infections observed in six NHPs. The contribution of these secondary infections to disease outcome cannot be discerned in this study, but bacterial infection may have exacerbated lymphoid necrosis and depletion, bone marrow disruption, skin and GI tract lesions. CPXV-induced damage to the GI mucosa could increase intestinal mucosal permeability leading to bacteria accessing the circulatory system. Similarly, loss of integrity of skin and oral mucosa also invites invasion of bacteria. Gram positive and gram negative bacteria were observed in the blood vessels and tissues, but no further identification was attempted. Secondary bacterial infections, notably by hemolytic streptococci in human smallpox (Kempton and Parsons, 1920), have been reported as complicating factors in humans with monkeypox and smallpox (Bras, 1952; Dixon, 1962; Jezek et al., 1987a; Martin, 2002) and experimental MPXV-induced disease (Johnson et al., 2011; Saijo et al., 2009; Zaucha et al., 2001).

Of the types of smallpox, hemorrhagic smallpox was rare but the most severe with the highest case fatality rate (Fenner, 1988a; Rao, 1964). This hemorrhagic CPXV model closely parallels human hemorrhagic smallpox and the VARV NHP model of hemorrhagic smallpox indicating that further studies of CPXV pathogenesis are warranted. As CPXV is a BSL-2 pathogen, this model could be used more widely to develop countermeasures that could then be tested against VARV in compliance with the FDA animal rule (Chapman et al., 2010; Lane and Poland, 2011; McFadden, 2010). Furthermore, the uncertain future of VARV research necessitates additional development of this CPXV and

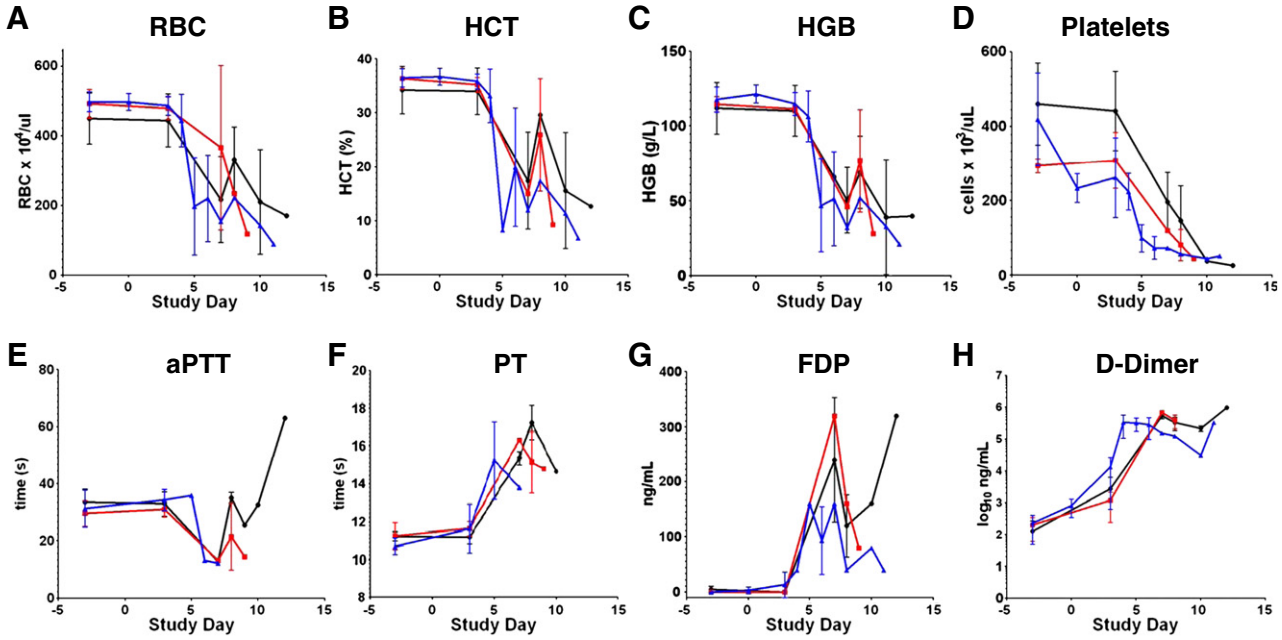

Fig. 4. Hematology supports a consumptive coagulopathy. (A) Red blood cell count, (B) hematocrit, (C) hemoglobin, (D) platelets, (E) activated partial thromboplastin time (aPTT), (F) prothrombin time (PT), (G) fibrin degradation products (FDP), and (H) D-dimer measured at times of periodic blood draw and necropsy. Black line represents 5×10^5 PFU group (n=4), red line represents 5×10^6 PFU group (n=4), and blue line represents 5×10^7 PFU group (n=6) except for aPTT and PT where the 5×10^7 PFU group has an n of 3. Bars represent standard deviation.

other orthopoxvirus models (Lane and Poland, 2011; McFadden, 2010). Studies to determine if inoculation of NHPs with a lower dose of CPXV would result in more classical poxviral disease with lesser hemorrhagic signs and increased lesion development are ongoing. Additionally, exploration of other inoculation routes is warranted as this study and IV inoculation represent the first steps in investigation of CPXV in macaques as an alternate model of orthopoxvirus disease. Future studies will also aim to identify viral and host factors which lead to hemorrhagic poxviral disease and lethality. The cause of death from human hemorrhagic smallpox was often referred to as toxemia or more recently a cytokine storm (Councilman et al., 1904a; Fenner, 1988b; Jahrling et al., 2004; Martin, 2002; Ricketts, 1910). However, toxemia was poorly defined due to technological limitations and the exact cause of death remains unknown. The mechanism by which VARV manifested as a hemorrhagic disease rather than classical smallpox is also unknown, but likely involves a combination of multi-organ system failure, coagulopathy, dysregulation of the cytokine response, immune system compromise, and opportunistic bacterial infections. Further development of this model may identify viral and host factors leading to hemorrhagic disease and aid therapeutic development.

Materials and methods

Virus and cells

CPXV Brighton Red strain was propagated in Vero E6 cells at a multiplicity of infection (MOI) of 0.1 for 7 days. Virus was then pelleted over 36% sucrose at 25,000 rpm in a SW32ti rotor for 80 min at 4 °C. The virus was kindly provided by Dr. Grant McFadden, University of Florida. Vero E6 cells were maintained in Dulbecco's modified Eagle's medium (DMEM) (HyClone, Logan, UT) supplemented with 10% fetal bovine serum (FBS) (HyClone, Logan, UT) and 1% penicillin/streptomycin at 37 °C with 5% CO_2. BSC-1 cells were maintained in minimum essential medium (MEM) supplemented with 10% FBS and 1% penicillin and streptomycin at 37 °C with 5% CO_2. Inocula were prepared by disruption of Vero E6 cells in an Ultrasonic Processor VCX-750 (Sonics and Materials, Newtown CT) for 120 s at 40% power on ice followed by centrifugation at 500 *g* for 10 min at 4 °C.

Challenge and monitoring of NHPs

Prior to enrollment, cynomolgus macaques (*M. fascicularis*), were screened for simian retrovirus (SRV), simian T-lymphotrophic virus (STLV), MPXV, vaccinia virus (VACV), and CPXV by quantitative polymerase chain reaction (qPCR). Selected NHPs ranged in weight from 2.7 to 4.2 kg. NHPs were also screened for detectable neutralizing antibody activity against VACV. All animal procedures were approved by the National Institute of Allergy and Infectious Diseases Animal Care and Use Committee and adhered to National Institutes of Health (NIH) policies including those set forth in the Guide for the Care and Use of Laboratory Animals.

For IV inoculation, NHPs were anesthetized with Telazol® (combination of tiletamine and zolazepam), and 1 mL of CPXV virus inoculum was injected into the saphenous vein with a 21-gauge needle. Two independent experiments were performed. In the pilot experiment, 3 NHPs were inoculated with 5×10^7 PFU and physical exams, including temperature, body weight, and lesion counts, were performed. Peripheral blood and oral and nasal swabs were collected on days 0, 4, 8, 10, and 12 post-inoculation. In the second experiment, 3 groups of NHPs were inoculated with serial 10-fold dilutions of CPXV; 5×10^7 PFU (n = 3), 5×10^6 PFU (n = 4), and 5×10^5 PFU (n = 4). Physical exams were performed and samples were collected in the same manner as the first experiment on days −3, 3, 8, 10, and 12 post-inoculation. NHPs were monitored at least twice daily. A pre-established scale was used to monitor clinical endpoint criteria that included scoring of (1) overall clinical appearance, (2) respiratory abnormalities, (3) activity and behavior, (4) responsiveness, and (5) core body temperatures. Moribund clinical endpoint criteria were considered met and NHPs euthanized when clinical signs including uncontrolled epistaxis, melena, retrobulbar hemorrhage, respiratory distress, severe recumbency, non-responsiveness, and hypothermia were observed.

Hematology and serology

Complete blood counts including leukocyte differentials (CBC/diff) were determined from blood samples collected in ethylenediaminetetraacetic acid (EDTA)-coated blood tubes and analyzed using a Sysmex XS1000i™ (Sysmex America, Mundelein, IL). To further analyze

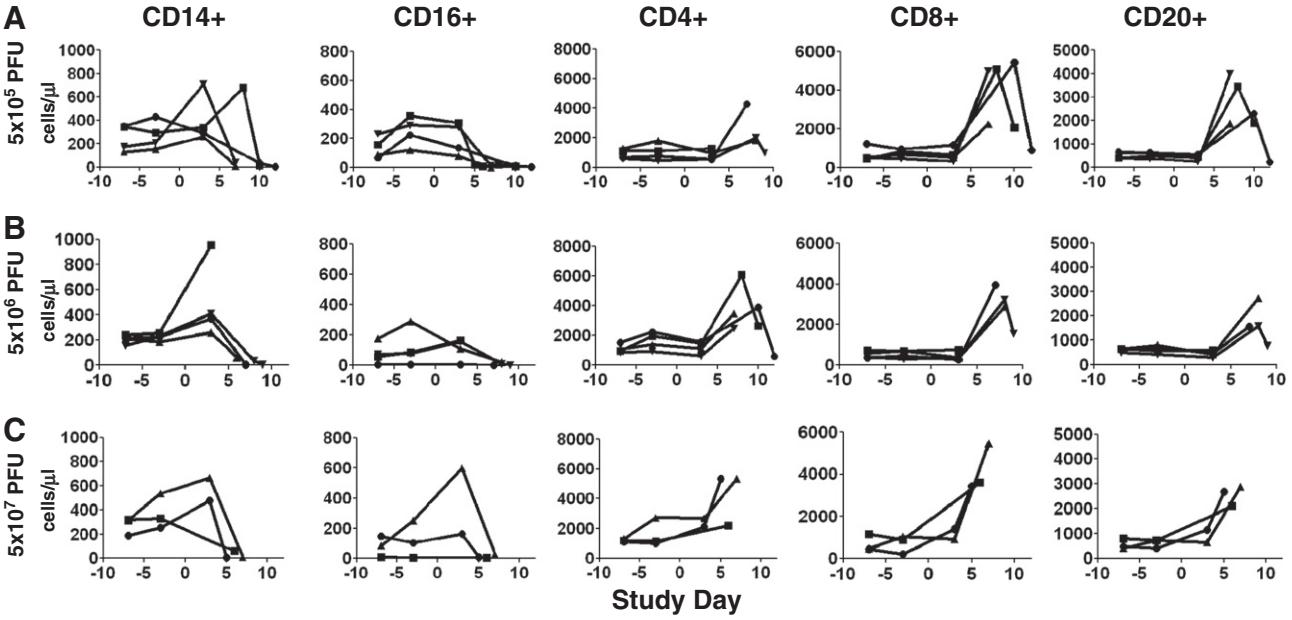

Fig. 5. Changes in PBMC concentrations after CPXV infection. Various PBMC cell populations were assayed periodically by TruCount analysis as described in the Materials and methods. Lines represent individual NHPs. (A) 5×10^5 PFU group (n = 4), (B) 5×10^6 PFU group (n = 4), and (C) 5×10^7 PFU group (n = 3).

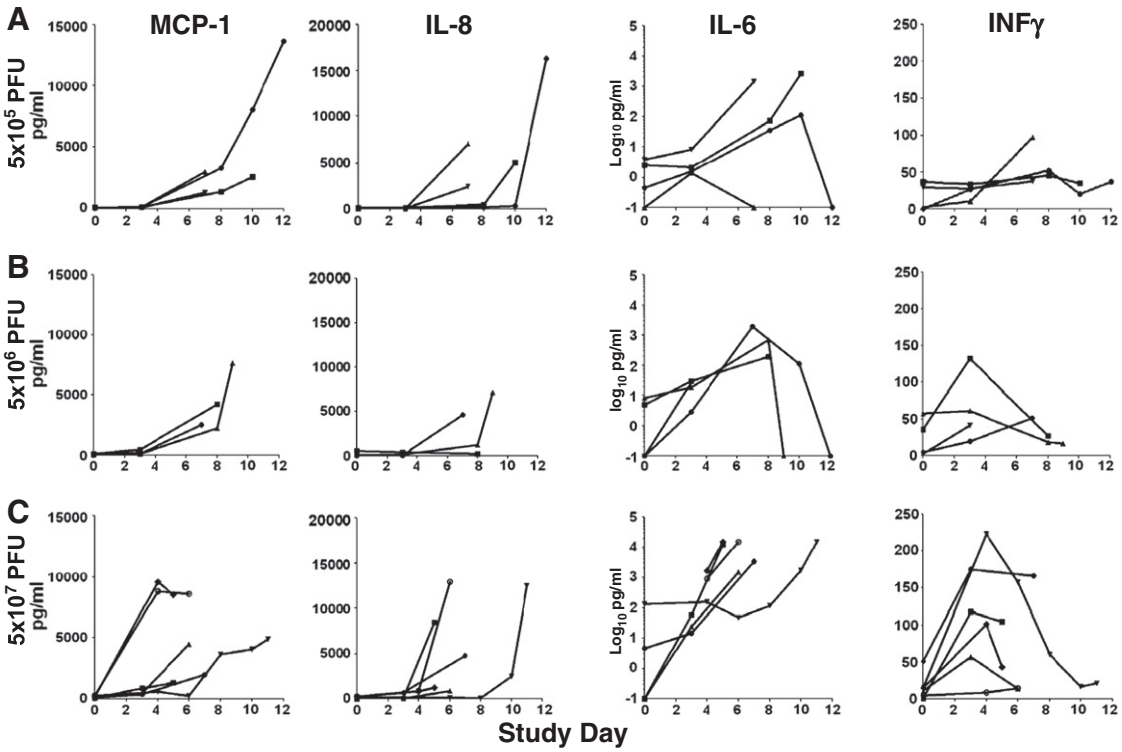

Fig. 6. Changes in cytokine/chemokine concentrations after CPXV infection. Plasma levels of the indicated factors were assayed periodically as described in the Materials and methods. Lines represent individual NHPs. (A) 5×10^5 PFU group (n = 4), (B) 5×10^6 PFU group (n = 4), and (C) 5×10^7 PFU group (n = 6).

peripheral blood mononuclear cells (PBMCs), EDTA whole blood samples were collected from NHPs and analyzed using TruCount™ tubes (BD Biosciences, San Jose, CA). A commercial antibody cocktail containing markers for CD45, CD3, CD4, CD8, CD14, CD16, and CD20 (BD Biosciences, San Jose, CA) was brought up to a volume of 50 μL in phosphate buffered saline (PBS) plus 2% fetal bovine serum (FBS) and 50 μL of cocktail was transferred into a TruCount™ tube. Fifty microliters of EDTA whole blood was then added to the tube, gently mixed by vortex and incubated for 20 min at room temperature. Samples were fixed using BD FACS Lysis Buffer (BD Biosciences San Jose, CA) and then analyzed on the BD Fortessa Flow Cytometer. Data were analyzed using FlowJo analysis software v8.6.3 (TreeStar Inc., Ashland OR). Cells were first gated on CD45, then CD3+ and CD3− populations were selected against CD45. CD3+ populations were then gated against CD4 and CD8 subpopulations. CD3− populations were gated against CD14, CD16 and CD20 subpopulations.

For coagulation studies, samples were analyzed on a Thromboscreen 2000 (Pacific Hemostasis and Fisher Scientific Diagnostics, Middletown, VA) to determine activated partial thromboplastin time (aPTT) and prothrombin time (PT). The concentration of D-dimers and fibrin degradation products (FDPs) was assayed from citrate-treated blood samples using an enzyme-linked immunosorbent assay (ELISA) according to the manufacturer's directions (Diagnostica Stago, Parsippany, NJ).

Quantification of viremia by quantitative PCR

Viral load in whole blood was determined by quantitative PCR as described previously (Kulesh et al., 2004). Briefly, DNA was isolated

Table 2
Additional cytokines/chemokines with increased plasma concentrations.

Cytokine/ chemokine	Dose (PFU)	Mean day of cytokine peak (range)	Mean peak concentration (pg/mL) (range)	Mean fold change from day zero	No. of NHPs with peak concentrations at endpoint
IL-1-ra	5×10^5	9 (7–12)	8878 (6163–11,596)	6268	4/4
	5×10^6	6.75 (3–9)	4537 (41–9419)	3645	3/3
	5×10^7	6.67 (5–11)	9355 (7445–10,282)	4664	6/6
IL-18	5×10^5	9 (7–12)	715 (84–2458)	715	4/4
	5×10^6	5.5 (3–9)	351 (60–683)	351	2/3
	5×10^7	5.17 (3–11)	691 (30–2396)	314	3/6
RANTES	5×10^5	3.25 (2–7)	6072 (2567–14,760)	7	1/4
	5×10^6	2.5 (0–9)	4890 (1289–12,107)	3	2/3
	5×10^7	3.17 (0–11)	8325 (1786–17,517)	3	2/6
VEGF	5×10^5	9 (7–12)	225 (64–279)	225	1/4
	5×10^6	5.5 (3–9)	438 (43–1304)	438	2/3
	5×10^7	6.67 (5–11)	763 (113–1544)	584	6/6
sCD40L	5×10^5	2.5 (0–7)	199 (55–289)	5	1/4
	5×10^6	2.5 (0–7)	263 (83–462)	2	1/3
	5×10^7	1.33 (0–5)	204 (84–530)	322	1/6
G-CSF	5×10^5	8.5 (7–10)	716 (175–1501)	344	3/4
	5×10^6	6.75 (3–9)	2639 (49–6391)	98	3/3
	5×10^7	6.67 (5–11)	3250 (344–7591)	39	6/6

Table 3
Viral load in blood and in oral and nasal swabs.

Dose (PFU)	Group size	Viremia		Oral swab		Nasal swab	
		Mean peak (log_{10} gene copy/mL) (range)	Mean day of peak (range)	Mean peak (log_{10} PFU/mL) (range)	Mean day of peak (range)	Mean peak (log_{10} PFU/mL) (range)	Mean day of peak (range)
5×10^5	4	8.6 (8.5–8.7)	8.5 (7–12)	3.6 (2.6–4.0)	8.5 (7–12)	3.3 (2.0–3.7)	7.5 (7–8)
5×10^6	4	8.4 (5.0–8.8)	6.8 (3–9)	2.5 (2.0–3.0)	6 (3–8)	6.3 (2.0–6.7)	6.5 (3–8)
5×10^7	6	9.1 (8.2–9.8)	6.0 (4–10)	2.9 (2.5–3.3)	4.2 (4–7)	5.9 (3.2–6.4)	6.5 (4–11)

using Genfind v2 according to manufacturer's directions (Agencourt, Danvers MA) and isolated DNA was screened for the presence of CPXV using primers specific for the HA gene (Sofi Ibrahim et al., 2003) and a LightCycler apparatus (Roche, Basel Switzerland). The limit of detection was 10 gene copies/mL.

Plaque assay

The concentration of infectious CPXV in oral and nasal swabs and tissue samples was determined by plaque assay on BSC-1 cell monolayers. Swabs were placed in 1 mL of sterile 1× PBS, soaked for 30 s, and stored at −80 °C. Swab suspensions were thawed and sonicated for 120 s on ice, serially diluted 10-fold, and then added to confluent BSC-1 cells. Forty one tissues from each NHP were evaluated, and the tissues with the highest and most consistent levels of virus replication are described below. Tissue samples were excised during necropsy, flash frozen, and stored at −80 °C. Tissues were homogenized (10% or 20% w/v), and 10-fold serial dilutions were incubated on confluent BSC-1 cells with a 0.8% agarose: MEM2% FBS overlay. Following incubation, agarose plugs were removed, the monolayers were stained with crystal violet (0.1% crystal violet, 20% ethanol v/v), and plaques were enumerated. Viral titers for the lymph nodes were the average of cervical, axillary, bronchial, mesenteric, inguinal, and popliteal lymph node titers. Bone marrow titers were the average of sternal, ilial, and femoral bone marrow titers. Viral loads in lungs were the average titers of samples from the 6 lobes for each NHP. CNS titers were the average of cerebrum, cerebellum, cervical spinal cord, thoracic spinal cord, and lumbar spinal cord titers. Liver titers were the average of left, right, medial, and caudal liver lobe titers. Ovary, kidney and adrenal gland titers were the average of both ovaries, kidneys, and adrenal gland titers.

Cytokine and chemokine analysis

The concentrations of 23 cytokines and chemokines in serum samples were analyzed using the Millipore Non-Human Primate Cytokine Panel Premixed 23-plex (Millipore Billerica MA). Plasma samples were transferred to a 96-well plate and incubated with antibody-coated beads directed against different cytokines or chemokines. For the chemokine Regulated upon Activation, Normal T-cell Expressed, and Secreted (RANTES) or CCL5, a 1:100 dilution was made for each sample. Following incubation, the beads were washed, incubated with anti-cytokine and chemokine antibodies, and incubated with Streptavidin-R-phycoerythrin (SAV/RPE). Beads were assayed on the Luminex 100/200 System (Bio-Rad, Hercules CA). Cytokines were included for comparison when there was a twofold or greater change above background detection of the manufacturer supplied standards for any NHP within a group.

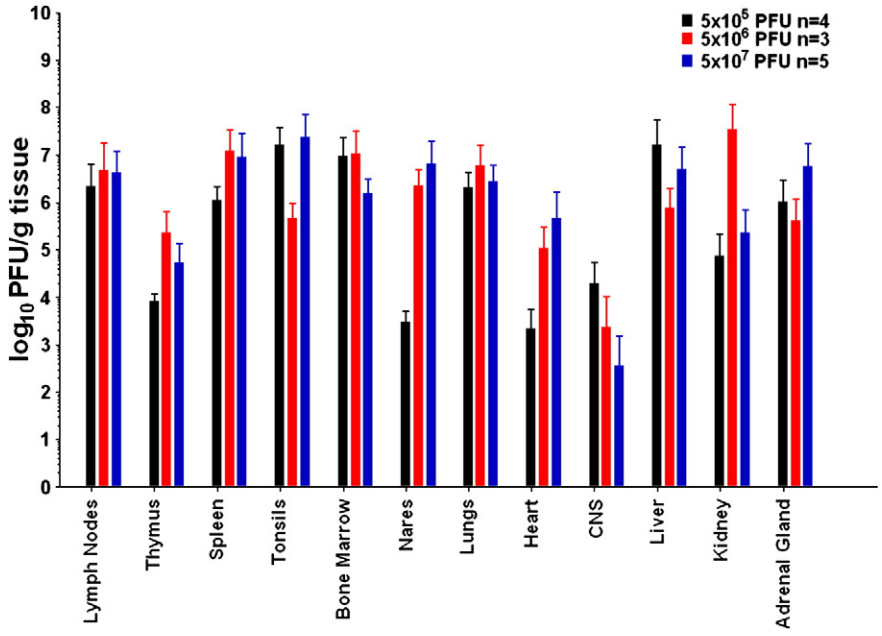

Fig. 7. CPXV demonstrated wide tissue distribution. At necropsy, tissue samples were homogenized and assayed for the presence of virus by plaque assay on BSC-1 cells. Mean virus titers are indicated for each tissue. Viral titers for the lymph nodes are the mean of cervical axillary, bronchial, mesenteric, inguinal, and popliteal lymph nodes. Bone marrow values are the mean of sternal, ilial, and femoral bone marrow samples. Viral loads in lungs are the mean titers of samples from the 6 lobes for each NHP. CNS is the mean of cerebrum, cerebellum, cervical spinal cord, thoracic spinal cord, and lumbar spinal cord. Liver titers are the mean of left, right, medial, and caudal liver lobes. Ovary, kidney and adrenal gland titers are the mean of both ovaries, kidneys and adrenal glands. Bars represent standard deviation.

Postmortem examination, histopathology and immunohistochemistry

All animals except one were necropsied on the day of death, and gross lesions were recorded. One animal in the 5×10^6 PFU group was not necropsied, and the reporting of this group is reflected as $n=3$ when appropriate. Blood samples and oral and nasal swabs were collected. Tissues from all major organ systems were collected and fixed in 10% neutral buffered formalin, embedded in paraffin, sectioned at 5 μm, and stained with hematoxylin and eosin (H&E) according to established protocols. Separate tissue samples were collected and flash frozen for viral plaque assay as described above.

Immunohistochemistry (IHC) was performed on 5 μm thick sections of formalin-fixed paraffin embedded tissue using the Bond automated immunostainer (Leica Microsystems, Bannockburn, IL). Paraffin was removed with xylene, and the sections were rehydrated in a series of alcohol washes. Heat-induced epitope retrieval was performed using citrate (pH 6.0) at 100 °C for 25 min. Orthopoxvirus antigen was identified immunohistochemically using a biotinylated rabbit anti-vaccinia virus polyclonal antibody (1:2000; Catalog #YVS8101, Accurate Chemical, Westbury, NY) incubated for 15 min at room temperature. Primary antibody was localized with horseradish peroxidase and diaminobenzidine substrate. In negative controls, buffer was used in place of the primary antibody. Sections were counterstained with hematoxylin and examined by light microscopy by two veterinary pathologists (AJJ, SY).

Acknowledgments

This work, in part, was supported by the NIAID Division of Intramural Research. We are grateful to Sharon Altmann, Catherine Jett, Haifeng Song, Kurt Cooper, Marisa St. Claire, Russell Byrum, and Dan Ragland for their contributions to these studies. We thank Marisa St. Claire, Laura Bollinger and Fabian De Kok Mercado for their contribution to the preparation of this manuscript. We thank Grant McFadden University of Florida for providing Cowpox Brighton Red.

References

Anon., 2009. Annual Report to Congress. Department of Defense, Chemical and Biological Defense Program. .

Baxby, D., Bennett, M., Getty, B., 1994. Human cowpox 1969–93: a review based on 54 cases. Br. J. Dermatol. 131, 598–607.

Bras, G., 1952. The morbid anatomy of smallpox. Doc. Med. Geogr. Trop. 4, 303–351.

Bray, M., Buller, M., 2004. Looking back at smallpox. Clin. Infect. Dis. 38, 882–889.

Chapman, J.L., Nichols, D.K., Martinez, M.J., Raymond, J.W., 2010. Animal models of orthopoxvirus infection. Vet. Pathol. 47, 852–870.

Charo, I.F., Taubman, M.B., 2004. Chemokines in the pathogenesis of vascular disease. Circ. Res. 95, 858–866.

Chen, N., Li, G., Liszewski, M.K., Atkinson, J.P., Jahrling, P.B., Feng, Z., Schriewer, J., Buck, C., Wang, C., Lefkowitz, E.J., Esposito, J.J., Harms, T., Damon, I.K., Roper, R.L., Upton, C., Buller, R.M., 2005. Virulence differences between monkeypox virus isolates from West Africa and the Congo basin. Virology 340, 46–63.

Councilman, W.T., Magrath, G.B., Brinckerhoff, W.R., 1904a. The pathological anatomy and histology of variola. J. Med. Res. 11, 12–135.

Councilman, W.T., Magrath, G.B., Brinckerhoff, W.R., 1904b. The pathological anatomy and histology of variola. J. Med. Res. 11, 12–135.

Dixon, C.W., 1962. Smallpox. Churchill, London.

Downie, A.W., Fedson, D.S., Saint Vincent, L., Rao, A.R., Kempe, C.H., 1969. Haemorrhagic smallpox. J. Hyg. (Lond) 67, 619–629.

Earl, P.L., Americo, J.L., Wyatt, L.S., Eller, L.A., Whitbeck, J.C., Cohen, G.H., Eisenberg, R.J., Hartmann, C.J., Jackson, D.L., Kulesh, D.A., Martinez, M.J., Miller, D.M., Mucker, E.M., Shamblin, J.D., Zwiers, S.H., Huggins, J.W., Jahrling, P.B., Moss, B., 2004. Immunogenicity of a highly attenuated MVA smallpox vaccine and protection against monkeypox. Nature 428, 182–185.

Earl, P.L., Americo, J.L., Wyatt, L.S., Anne Eller, L., Montefiori, D.C., Byrum, R., Piatak, M., Lifson, J.D., Rao Amara, R., Robinson, H.L., Huggins, J.W., Moss, B., 2007. Recombinant modified vaccinia virus Ankara provides durable protection against disease caused by an immunodeficiency virus as well as long-term immunity to an orthopoxvirus in a non-human primate. Virology 366 (1), 84–97.

Earl, P.L., Americo, J.L., Wyatt, L.S., Espenshade, O., Bassler, J., Gong, K., Lin, S., Peters, E., Rhodes Jr., L., Spano, Y.E., Silvera, P.M., Moss, B., 2008. Rapid protection in a monkeypox model by a single injection of a replication-deficient vaccinia virus. Proc. Natl. Acad. Sci. U. S. A. 105, 10889–10894.

Edghill-Smith, Y., Bray, M., Whitehouse, C.A., Miller, D., Mucker, E., Manischewitz, J., King, L.R., Robert-Guroff, M., Hryniewicz, A., Venzon, D., Meseda, C., Weir, J., Nalca, A., Livingston, V., Wells, J., Lewis, M.G., Huggins, J., Zwiers, S.H., Golding, H., Franchini, G., 2005a. Smallpox vaccine does not protect macaques with AIDS from a lethal monkeypox virus challenge. J. Infect. Dis. 191, 372–381.

Edghill-Smith, Y., Golding, H., Manischewitz, J., King, L.R., Scott, D., Bray, M., Nalca, A., Hooper, J.W., Whitehouse, C.A., Schmitz, J.E., Reimann, K.A., Franchini, G., 2005b. Smallpox vaccine-induced antibodies are necessary and sufficient for protection against monkeypox virus. Nat. Med. 11, 740–747.

Favaloro, E.J., 2010. Laboratory testing in disseminated intravascular coagulation. Semin. Thromb. Hemost. 36, 458–467.

Fenner, F., 1988a. The clinical features of smallpox. In: Fenner, F., Henderson, D.A., Arita, I., Jezek, Z., Ladnyi, I.D. (Eds.), Smallpox and Its Eradication. World Health Organization, Geneva.

Fenner, F., 1988b. The eradication of smallpox. Impact Sci. Soc. 38, 147–158.

Geisbert, T.W., Jahrling, P.B., 2004. Exotic emerging viral diseases: progress and challenges. Nat. Med. 10, S110–S121.

Goff, A.J., Chapman, J., Foster, C., Wlazlowski, C., Shamblin, J., Lin, K., Kreiselmeier, N., Mucker, E., Paragas, J., Lawler, J., Hensley, L., 2011. A novel respiratory model of infection with monkeypox virus in cynomolgus macaques. J. Virol. 85, 4898–4909.

Gubser, C., Hue, S., Kellam, P., Smith, G.L., 2004. Poxvirus genomes: a phylogenetic analysis. J. Gen. Virol. 85, 105–117.

Haviland, J.W., 1952. Purpura variolosa; its manifestations in skin and blood. Yale J. Biol. Med. 24, 518–524.

Hooper, J.W., Thompson, E., Wilhelmsen, C., Zimmerman, M., Ichou, M.A., Steffen, S.E., Schmaljohn, C.S., Schmaljohn, A.L., Jahrling, P.B., 2004. Smallpox DNA vaccine protects nonhuman primates against lethal monkeypox. J. Virol. 78, 4433–4443.

Huerta-Zepeda, A., Cabello-Gutierrez, C., Cime-Castillo, J., Monroy-Martinez, V., Manjarrez-Zavala, M.E., Gutierrez-Rodriguez, M., Izaguirre, R., Ruiz-Ordaz, B.H., 2008. Crosstalk between coagulation and inflammation during Dengue virus infection. Thromb. Haemost. 99, 936–943.

Huggins, J., Goff, A., Hensley, L., Mucker, E., Shamblin, J., Wlazlowski, C., Johnson, W., Chapman, J., Larsen, T., Twenhafel, N., Karem, K., Damon, I.K., Byrd, C.M., Bolken, T.C., Jordan, R., Hruby, D., 2009. Nonhuman primates are protected from smallpox virus or monkeypox virus challenges by the antiviral drug ST-246. Antimicrob. Agents Chemother. 53, 2620–2625.

Hutchinson, K.L., Rollin, P.E., 2007. Cytokine and chemokine expression in humans infected with Sudan Ebola virus. J. Infect. Dis. 196 (Suppl. 2), S357–S363.

Jahrling, P.B., Hensley, L.E., Martinez, M.J., Leduc, J.W., Rubins, K.H., Relman, D.A., Huggins, J.W., 2004. Exploring the potential of variola virus infection of cynomolgus macaques as a model for human smallpox. Proc. Natl. Acad. Sci. U. S. A. 101, 15196–15200.

Jahrling, P.B., Fritz, E.A., Hensley, L.E., 2005. Countermeasures to the bioterrorist threat of smallpox. Curr. Mol. Med. 5, 817–826.

Jezek, Z., Gromyko, A.I., Szczeniowski, M.V., 1983. Human monkeypox. J. Hyg. Epidemiol. Microbiol. Immunol. 27, 13–28.

Jezek, Z., Grab, B., Dixon, H., 1987a. Stochastic model for interhuman spread of monkeypox. Am. J. Epidemiol. 126, 1082–1092.

Jezek, Z., Szczeniowski, M., Paluku, K.M., Mutombo, M., 1987b. Human monkeypox: clinical features of 282 patients. J. Infect. Dis. 156, 293–298.

Jezek, Z., Grab, B., Szczeniowski, M.V., Paluku, K.M., Mutombo, M., 1988. Human monkeypox: secondary attack rates. Bull. World Health Organ. 66, 465–470.

Johnson, K., Choi, Y., DeGroot, E., Samuels, I., Creasey, A., Aarden, L., 1998. Potential mechanisms for a proinflammatory vascular cytokine response to coagulation activation. J. Immunol. 160, 5130–5135.

Johnson, R.F., Dyall, J., Ragland, D.R., Huzella, L., Byrum, R., Jett, C., St Claire, M., Smith, A.L., Paragas, J., Blaney, J.E., Jahrling, P.B., 2011. Comparative analysis of monkeypox virus infection of cynomolgus macaques by the intravenous or intrabronchial inoculation route. J. Virol. 85, 2112–2125.

Jordan, R., Goff, A., Frimm, A., Corrado, M.L., Hensley, L.E., Byrd, C.M., Mucker, E., Shamblin, J., Bolken, T.C., Wlazlowski, C., Johnson, W., Chapman, J., Twenhafel, N., Tyavanagimatt, S., Amantana, A., Chinsangaram, J., Hruby, D.E., Huggins, J., 2009. ST-246 antiviral efficacy in a nonhuman primate monkeypox model: determination of the minimal effective dose and human dose justification. Antimicrob. Agents Chemother. 53, 1817–1822.

Kempton, R.M., Parsons, J.P., 1920. Report of a case of hemorrhagic smallpox: a consideration of the role played by the hemolytic *Streptococcus*. Arch. Intern. Med. 26, 594–600.

Kramski, M., Matz-Rensing, K., Stahl-Hennig, C., Kaup, F.J., Nitsche, A., Pauli, G., Ellerbrok, H., 2010. A novel highly reproducible and lethal nonhuman primate model for orthopox virus infection. PLoS One 5, e10412.

Kulesh, D.A., Loveless, B.M., Norwood, D., Garrison, J., Whitehouse, C.A., Hartmann, C., Mucker, E., Miller, D., Wasieloski Jr., L.P., Huggins, J., Huhn, G., Miser, L.L., Imig, C., Martinez, M., Larsen, T., Rossi, C.A., Ludwig, G.V., 2004. Monkeypox virus detection in rodents using real-time 3′-minor groove binder TaqMan assays on the Roche LightCycler. Laboratory investigation. J. Tech. Methods Pathol. 84, 1200–1208.

Lane, J.M., Poland, G.A., 2011. Why not destroy the remaining smallpox virus stocks? Vaccine 29, 2823–2824.

Lefkowitz, E.J., Upton, C., Changayil, S.S., Buck, C., Traktman, P., Buller, R.M., 2005. Poxvirus Bioinformatics Resource Center: a comprehensive Poxviridae informational and analytical resource. Nucleic Acids Res. 33, D311–D316.

Levi, M., van der Poll, T., 2010. Inflammation and coagulation. Crit Care Med. 38, S26–34.

Likos, A.M., Sammons, S.A., Olson, V.A., Frace, A.M., Li, Y., Olsen-Rasmussen, M., Davidson, W., Galloway, R., Khristova, M.L., Reynolds, M.G., Zhao, H., Carroll, D.S., Curns, A., Formenty, P., Esposito, J.J., Regnery, R.L., Damon, I.K., 2005. A tale of two clades: monkeypox viruses. J. Gen. Virol. 86, 2661–2672.

Lillie, R.D., 1930. Smallpox and vaccinia: the pathologic histology. Arch. Pathol. 10, 241–291.

Martin, D.B., 2002. The cause of death in smallpox: an examination of the pathology record. Mil. Med. 167, 546–551.

Martina, B.E., van Doornum, G., Dorrestein, G.M., Niesters, H.G., Stittelaar, K.J., Wolters, M.A., van Bolhuis, H.G., Osterhaus, A.D., 2006. Cowpox virus transmission from rats to monkeys, the Netherlands. Emerg. Infect. Dis. 12, 1005–1007.
Matz-Rensing, K., Ellerbrok, H., Ehlers, B., Pauli, G., Floto, A., Alex, M., Czerny, C.P., Kaup, F.J., 2006. Fatal poxvirus outbreak in a colony of New World monkeys. Vet. Pathol. 43, 212–218.
McFadden, G., 2010. Killing a killer: what next for smallpox? PLoS pathog. 6, e1000727.
McKenzie, P.J., Githens, J.H., Harwood, M.E., Roberts, J.F., Rao, A.R., Kempe, C.H., 1965. Haemorrhagic smallpox. 2. Specific bleeding and coagulation studies. Bull. World Health Organ. 33, 773–782.
Parker, S., Nuara, A., Buller, R.M., Schultz, D.A., 2007. Human monkeypox: an emerging zoonotic disease. Future Microbiol. 2, 17–34.
Rao, A.R., 1964. Haemorrhagic smallpox: a study of 240 cases. J. Indian Med. Assoc. 43, 224–229.
Ricketts, T.F., 1910. The Diagnosis of Smallpox. Funk and Wagnalls, New York.
Rimoin, A.W., Mulembakani, P.M., Johnston, S.C., Smith, J.O., Kisalu, N.K., Kinkela, T.L., Blumberg, S., Thomassen, H.A., Pike, B.L., Fair, J.N., Wolfe, N.D., Shongo, R.L., Graham, B.S., Formenty, P., Okitolonda, E., Hensley, L.E., Meyer, H., Wright, L.L., Muyembe, J.J., 2010. Major increase in human monkeypox incidence 30 years after smallpox vaccination campaigns cease in the Democratic Republic of Congo. Proc. Natl. Acad. Sci. U. S. A.
Roberts, J.F., Coffee, G., Creel, S.M., Gaal, A., Githens, J.H., Rao, A.R., Sundara Babu, B.V., Kempe, C.H., 1965. Haemorrhagic smallpox. I. Preliminary haematological studies. Bull. World Health Organ. 33, 607–613.
Saijo, M., Ami, Y., Suzaki, Y., Nagata, N., Iwata, N., Hasegawa, H., Iizuka, I., Shiota, T., Sakai, K., Ogata, M., Fukushi, S., Mizutani, T., Sata, T., Kurata, T., Kurane, I., Morikawa, S., 2009. Virulence and pathophysiology of the Congo Basin and West African strains of monkeypox virus in non-human primates. J. Gen. Virol. 90, 2266–2271.
Sbrana, E., Jordan, R., Hruby, D.E., Mateo, R.I., Xiao, S.Y., Siirin, M., Newman, P.C., AP, D.A. R., Tesh, R.B., 2007. Efficacy of the antipoxvirus compound ST-246 for treatment of severe orthopoxvirus infection. Am. J. Trop. Med. Hyg. 76, 768–773.
Seet, B.T., Johnston, J.B., Brunetti, C.R., Barrett, J.W., Everett, H., Cameron, C., Sypula, J., Nazarian, S.H., Lucas, A., McFadden, G., 2003. Poxviruses and immune evasion. Annu. Rev. Immunol. 21, 377–423.
Smee, D.F., Gowen, B.B., Wandersee, M.K., Wong, M.H., Skirpstunas, R.T., Baldwin, T.J., Hoopes, J.D., Sidwell, R.W., 2008. Differential pathogenesis of cowpox virus intranasal infections in mice induced by low and high inoculum volumes and effects of cidofovir treatment. Int. J. Antimicrob. Agents 31, 352–359.
Sofi Ibrahim, M., Kulesh, D.A., Saleh, S.S., Damon, I.K., Esposito, J.J., Schmaljohn, A.L., Jahrling, P.B., 2003. Real-time PCR assay to detect smallpox virus. J. Clin. Microbiol. 41, 3835–3839.
Stittelaar, K.J., Kuiken, T., de Swart, R.L., van Amerongen, G., Vos, H.W., Niesters, H.G., van Schalkwijk, P., van der Kwast, T., Wyatt, L.S., Moss, B., Osterhaus, A.D., 2001. Safety of modified vaccinia virus Ankara (MVA) in immune-suppressed macaques. Vaccine 19, 3700–3709.
Stittelaar, K.J., van Amerongen, G., Kondova, I., Kuiken, T., van Lavieren, R.F., Pistoor, F.H., Niesters, H.G., van Doornum, G., van der Zeijst, B.A., Mateo, L., Chaplin, P.J., Osterhaus, A.D., 2005. Modified vaccinia virus Ankara protects macaques against respiratory challenge with monkeypox virus. J. Virol. 79, 7845–7851.
Stittelaar, K.J., Neyts, J., Naesens, L., van Amerongen, G., van Lavieren, R.F., Holy, A., De Clercq, E., Niesters, H.G., Fries, E., Maas, C., Mulder, P.G., van der Zeijst, B.A., Osterhaus, A.D., 2006. Antiviral treatment is more effective than smallpox vaccination upon lethal monkeypox virus infection. Nature 439, 745–748.
Sullivan, N.J., Sanchez, A., Rollin, P.E., Yang, Z.Y., Nabel, G.J., 2000. Development of a preventive vaccine for Ebola virus infection in primates. Nature 408, 605–609.
Tucker, J.B., 2011. Breaking the deadlock over destruction of the smallpox virus stocks. Biosecur. Bioterror. 9, 55–67.
Vorou, R.M., Papavassiliou, V.G., Pierroutsakos, I.N., 2008. Cowpox virus infection: an emerging health threat. Curr. Opin. Infect. Dis. 21, 153–156.
Wauquier, N., Becquart, P., Padilla, C., Baize, S., Leroy, E.M., 2010. Human fatal zaire ebola virus infection is associated with an aberrant innate immunity and with massive lymphocyte apoptosis. PLoS Negl. Trop. Dis. 4 (10), e837.
Xing, K., Deng, R., Wang, J., Feng, J., Huang, M., Wang, X., 2006. Genome-based phylogeny of poxvirus. Intervirology 49, 207–214.
Zaucha, G.M., Jahrling, P.B., Geisbert, T.W., Swearengen, J.R., Hensley, L., 2001. The pathology of experimental aerosolized monkeypox virus infection in cynomolgus monkeys (*Macaca fascicularis*). Laboratory investigation. J. Tech. Methods Pathol. 81, 1581–1600.